Desalination and Water Treatment
www.deswater.com

(2014) 1–11

doi: 10.1080/19443994.2014.914449

Taylor & Francis
Taylor & Francis Group

Removal of methylene blue and acid orange 7 from aqueous solutions by activated carbon coated with zinc oxide (ZnO) nanoparticles: equilibrium, kinetic, and thermodynamic study

H. Nourmoradi[a], A.R. Ghiasvand[b], Z. Noorimotlagh[a,*]

[a]*Department of Environmental Health Engineering, School of Health, Ilam University of Medical Sciences, Pajouhesh Ave, Banganjab, Ilam, Iran, Tel. +988412235733; email: ilam_nourmoradi@yahoo.com (H. Nourmoradi), Tel./Fax: +988412235733; email: noorimotlagh.zahra@gmail.com (Z. Noorimotlagh)*

[b]*Faculty of Science, Department of Chemistry, Lorestan University, Khoramabad, Iran, Tel. +986612200185; email: a_ghiasvand@yahoo.com (A.R. Ghiasvand)*

Received 2 February 2014; Accepted 28 March 2014

ABSTRACT

Various industries like textile, plastic, pulp, and paper produce dye containing wastewaters that have harmful effects on the environment as well as human health. The aim of this study was to investigate the effect of granular activated carbon (AC) coated by zinc oxide nanoparticles (ZnO-np) in the removal of dyes, methylene blue (MB) and acid orange 7 (AO7), from aqueous solutions. The morphology of the AC and AC–ZnO was determined by SEM and the FTIR spectra confirmed the strong interaction between AC and ZnO. The effect of various parameters, such as nanoparticles loading onto the AC, pH, contact time, dye concentration, ion strength, temperature, and adsorbent regeneration, was studied on the adsorption. The results showed that the surface structure of the raw AC was porous and had irregular shapes, but the surface of the modified AC (AC–ZnO) due to the homogenous coating of the ZnO-np onto the AC was approximately uniform and regular. The sorption capacity and optimum contact time for the removal of MB (32.22 mg/g) and AO7 (32.13 mg/g) by AC–ZnO were obtained as 32.22 mg/g during 120 min and 32.13 mg/g over 150 min, respectively. The optimum pH for the sorption of MB occurred at pH 11 and for AO7 was obtained at pH 3. The results also showed that Langmuir isotherm and pseudo-second-order kinetic models fitted the experimental data better than other isotherm and kinetic models. It is obviously clear that AC–ZnO, in comparison with raw AC, was more efficient sorbent for the removal of MB and AO7 and it can be proposed for the removal of these dyes from aqueous solutions.

Keywords: Adsorption; Dye; Activated carbon; Zinc oxide nanoparticles; Aqueous solution

1. Introduction

In recent years, irregular industrial development has been considered as one of the major environmental problems, especially in developing countries [1]. Various industries including textile, plastic, pulp, and paper produce huge amounts of wastewater containing synthetic dyes [2]. Dyes used in these industries are generally classified as direct, reactive, acid, and

*Corresponding author.

basic dyes [3]. Dye-containing wastewaters have harmful effects on the aquatic environment as well as human health [4]. Methylene blue (MB) is a common basic dye that is used for dying clothes in textile industries [5]. MB can cause the adverse effects on human as cyanosis, vomiting, diarrhea, tachycardia, jaundice, etc. [5,6]. Acid Orange 7 (AO7) is another type of dye that is widely used in textile industries, because of its low cost and high solubility in water. AO7 is a toxic compound and its poor degradability in the environment can result in the presence of this dye for long time [7–9]. The removal of these dye substances from water and wastewater due to their detrimental effects is essential. Therefore, many treatment procedures including ion-exchange, reverse osmosis, adsorption, coagulation, membrane filtration, precipitation, advanced oxidation processes (ozonation and photo degradation), and biological methods have been applied to remove various dyes in the effluents [4,6,10,11]. Adsorption process, because of its simplicity, cost effective, and sorbent reusability, is an attractive alternative that has been extensively used to remove dyes from aqueous solutions [4,10,12]. It is now well documented that for the water and wastewater treatment, adsorption process has many advantages over other methods [13,14]. Moreover, the ability of adsorption to remove various toxic chemicals without producing any toxic byproducts, thus holding quality of water unchanged, has also popularized this treatment method in comparison to other above-mentioned processes [13]. Many studies have been conducted by different adsorbents such as activated carbon (AC) [15–20], peat [21], chitin [22], lime fly ash [23], rice husk [6], palygorskite clay [24], *rhizopus arrhizus* [25], swelling clay [26], clinoptilolite [27], water hyacinth [28], chitosan–zinc oxide nanoparticle [29], iron terephthalate [30], sawdust [31], palm kernel fiber [32], pineapple leaf powder [33], and perlite [34] for the removal of dyes from aqueous solutions. Adsorbents must have high specific surface area, sorption capacity, and active sites on their surfaces [35]. AC is the most frequently used sorbent that is applied for the removal of various dyes from the aqueous solutions [10]. Using materials like zinc oxide nanoparticles as a powerful sorbent on the surface of other adsorbents (e.g. AC) has many advantages [35,36]. This process can increase the number of sorption active sites onto the adsorbent, as well as the problems associated with the separation of the nanoparticles from the solution can be solved [35]. In the present work, zinc oxide nanoparticles (ZnO-np) was fixed onto AC to enhance its capacity for the sorption of dyes, MB and AO7. The effect of various parameters such as the nanoparticles loading, pH, contact time, dye concentration, ion strength, temperature, and its regeneration was studied on the adsorption.

2. Materials and methods

2.1. Materials

MB and AO7 dyes (>99% purity) were purchased from Merck Co (Darmstadt, Germany) and Alvan Sabet Co (Tehran, Iran), respectively. The chemical structure and general characteristics of the dyes are shown in Fig. 1 and Table 1, respectively. ZnO-np was provided by NanoAmor Co (USA). Other used chemicals including AC, HCl, and NaOH were also supplied from Merck Co (Darmstadt, Germany). The stock dye solutions (1,000 mg/L) were separately made by distilled water and kept at 4˚C. The working solutions were prepared through dilution of the stock solutions with distilled water.

2.2. Characterization and analysis

The morphology of the AC and AC–ZnO was determined by a scanning electron microscopy (SEM, Vega Tescan TS5136MM). The concentration of dyes in the solution was measured by an UV–vis spectrophotometer (DR-5000, Hach Co) at the maximum absorbance wavelength. The solution pH was determined by a pH meter (Metrohm Herisau Digital E 532).

2.3. Preparation and modification of the adsorbent

The AC was first ground and sieved into the particle sizes of range 0.15–0.5 mm. The grained AC was then washed with distilled water (four times) and

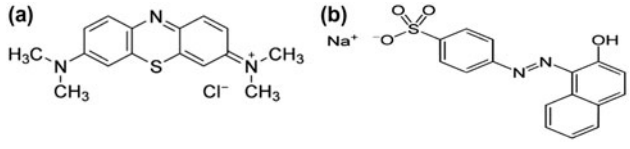

Fig. 1. Chemical structure of (a) MB and (b) AO7.

Table 1
General characteristics of MB and AO7

Characteristic	MB	AO7
Generic name	Methylene blue	Acid orange 7
Chemical formula	$C_{16}H_{18}N_3CLS$	$C_{16}H_{11}N_2NaO_4S$
Molecular weight (g/mol)	373.90	350.32
CAS number	7220-79-3	633-96-5
λ_{max} (nm)	665	485
Appearance	Sap green	Orange-red

dried at 90°C for 24 h. For the modification of AC, 0.01–0.5 g ZnO-np were separately dissolved in 50 mL distilled water and one gram of AC was added to it. The suspensions were mixed by an orbital shaker (250 rpm for 3 h) at room temperature (25°C) and filtered by filter paper (Whatman, No. 42). After that the modified AC was placed into a furnace at 250°C for 1 h. Finally, the adsorbent was cooled, washed with distilled water (four times), and dried (60°C for 24 h) for the experiments [36].

2.4. Adsorption experiments

The experiments were conducted in batch condition with 100 mL dye solution (50 mg/L) into a 200 mL conical flask at room temperature (25°C). The suspensions were mixed by a rotary shaker (250 rpm for 4 h), centrifuged (5,000 rpm for 5 min), and the clear supernatant was analyzed by UV–vis spectrophotometer. All experiments were carried out in triplicates and the average values were considered. The removal efficiency and sorption capacity of the sorbent were calculated by Eq. (1) and (2), respectively:

$$R\ (\%) = \frac{(C_0 - C_t)}{C_0} \times 100 \quad (1)$$

$$q_e = \frac{(C_0 - C_e)V}{m} \quad (2)$$

where R (%) and q_e (mg/g) are the removal efficiency and sorption capacity of the sorbent, respectively. C_0 (mg/L) is the initial dye concentration, C_e (mg/L) is the equilibrium dye concentration, m (g) is the sorbent mass, and V (L) is the volume of the dye solution [37,38].

2.4.1. Effect of the ZnO-np loading

The effect of different loading rates of ZnO-np onto the AC (0.01, 0.03, 0.05, 0.08, 0.1, 0.2, 0.3, 0.4, 0.5 g ZnO-np/g AC) for the removal of dye was investigated using 100 mL of the dye solution (50 mg/L) containing 0.15 g AC–ZnO at room temperature (25°C). The suspensions were mixed (4 h), centrifuged (5,000 rpm for 5 min), and analyzed for the dye through spectrophotometer.

2.4.2. Effect of contact time and pH

The effect of contact time on the dye sorption was conducted by 100 mL of the solution (50 mg/L) containing 0.15 g sorbent at different contact times (15, 30, 45, 60, 75, 90, 120, 150, 180, 210, and 240 min). The pH experiments were also carried out in the various pH values (3–11) with 0.15 g AC–ZnO into 100 mL of the dye solution (50 mg/L) at the optimum contact time. The adjustment of the solution pH was conducted by 0.1 M HCl and 0.1 M NaOH to the stated values. The contact time and pH samples were then centrifuged (5,000 rpm for 5 min) and analyzed for the dye through spectrophotometer.

2.4.3. Effect of adsorbate concentration and ion strength of solution

The effect of initial dye concentrations (10, 25, 50, 75, 100, 125, and 150 mg/L) on the adsorption was determined with 0.15 g AC–ZnO into 100 mL of dye solution (50 mg/L) at the optimum contact time and pH. The influence of ion strength, $CaCl_2$ (20, 40, 60, 80, and 100 mg/L of the Ca ion), on the adsorption was also performed using 0.15 g AC–ZnO into 100 mL of dye solution (50 mg/L) at optimum pH and contact time. The suspensions were then analyzed the same as above.

2.4.4. Effect of temperature

The effect of different temperatures (15, 25, 35, and 45°C) on the adsorption was performed by 0.15 g AC–ZnO into 100 mL of dye solution (50 mg/L) at the optimum contact time and pH. The suspensions were mixed and analyzed by UV–Vis.

2.4.5. Regeneration of dye saturated AC–ZnO

Regeneration of dye-saturated adsorbent was conducted through heating in distilled water, sulfuric acid, and sodium hydroxide solutions. The saturation of the adsorbent was conducted as follows: first, 0.15 g of the AC–ZnO was placed into 100 mL dye solution (50 mg/L) at the optimum contact time and pH with fixed temperature (25°C). After mixing, the suspension was centrifuged and the supernatant was analyzed. The saturated sorbent was then regenerated by the above-mentioned procedures. In order to determine the heating effect on the adsorbent regeneration, the amount of dye-saturated AC–ZnO was placed into a laboratory oven at 200°C for 60 min. To find out the effect of distilled water, sulfuric acid (10% v/v solution), and sodium hydroxide (10% v/v solution) on the regeneration, the amount of dye-saturated sorbent was separately placed into 100 mL of these solutions and mixed by orbital shaker (250 rpm for 30 min) in the room temperature (25°C). The adsorption experiments were then conducted by the regenerated adsorbent such as the original AC–ZnO.

3. Results and discussion

3.1. Characterization of the adsorbent

SEM studies provide useful information regarding the surface morphology of AC–ZnO structure. The SEM images of the AC and AC–ZnO are presented in Fig. 2. SE micrographs of the pure AC show that it is porous in nature with grain boundaries, Fig. 2(a). However, SE micrographs of AC–ZnO mixture reveal the surface texture and porosity nature (Fig. 2(b)). The immobilization of ZnO in the AC matrix partially blocked its pores, although the composite still displays a porous character with a large surface area. This is probably due to this fact that ZnO did not enter the inner microporosity of AC, resultant of the outer surfacing being most accessible. However, the pores of smaller sizes remained unblocked. FTIR spectra were recorded in order to understand the surface nature for the AC, ZnO, and AC–ZnO composite. The strong absorption band around 517 cm^{-1} (not shown) in Fig. 3(a) is related to the stretching vibrations of the Zn–O bonds. As shown in Fig. 3(a)), two peaks appear at around 3,440 and 1,630 cm^{-1} which correspond to the surface hydroxyl groups and physically adsorbed water molecules. Furthermore, in 1,600 cm^{-1}, a new band appeared corresponding to a C–O–C structure on the surface of the AC–ZnO composite [39]. However, AC has two broad bands in this region, due to the interaction of ZnO.

3.2. Effect of ZnO-np loading

The adsorption of MB and AO7 dyes by different loading rates of ZnO-np onto the AC is shown in Fig. 4. As seen, the removal efficiency (R) of both the dyes was quickly increased up to ZnO-np loading of 10 mg per one gram AC, and after that the sorption rate was nearly constant up to ZnO-np loading of 100 mg per one gram AC. The removal efficiency was then decreased at higher ZnO-np loading onto the AC (more than 100 mg ZnO-np/g AC). Decrease in the dye removal efficiency by AC–ZnO at the higher nanoparticles loading may be resulted from complete occupancy of the internal pores of the AC. The adsorbent with ZnO-np loading rate of 10 mg onto 1 g AC was used for the rest of the experiments in this study.

3.3. Effect of contact time

The adsorption process was examined to determine the optimum contact time at various times of 0–240 min. Fig. 5(a) shows the adsorption capacity of dyes by the adsorbent. As shown, the sorption rate was rapidly increased at the beginning of the sorption process (in the first 60 min). Then, the sorption was continued at a slower rate and finally reached saturation during 120 and 150 min for MB and AO7, respectively. The higher sorption value at the beginning of the process may be due to the presence of plenty of the adsorbent active sites in this stage. The sorption active sites were then diminished as the adsorption time goes forward [17]. The removal efficiency of MB and AO7 by AC–ZnO was obtained 96.66% (32.22 mg/g) and 96.4% (32.13 mg/g), respectively. Ozer et al. reported that the equilibrium contact time for the removal of MB by AC was achieved during 120 min with the sorption capacity of 37 mg/g (with initial dye concentration of 50 mg/L) [17]. Aber et al. also indicated that 96.24% of AO7 removal (with initial dye concentration of 150 mg/L) was obtained by powdered AC over the

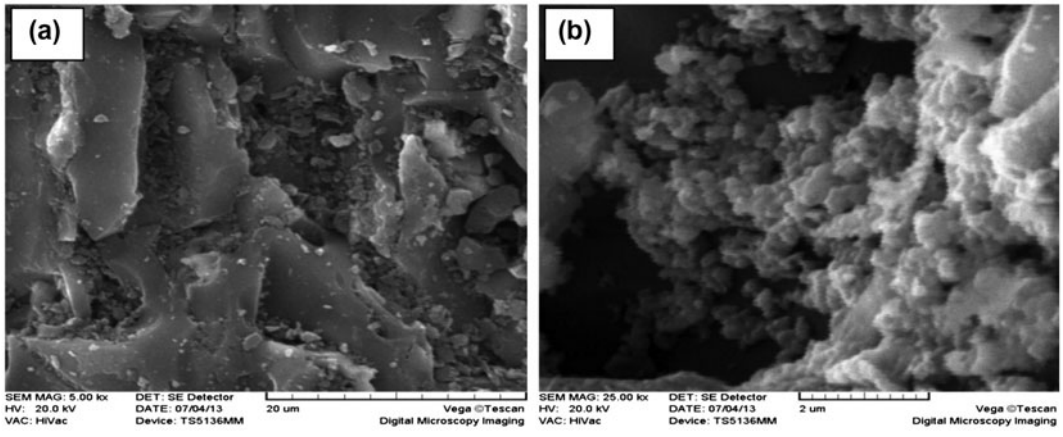

Fig. 2. The surface morphology of the adsorbent by SEM method for (a) AC and (b) AC–ZnO.

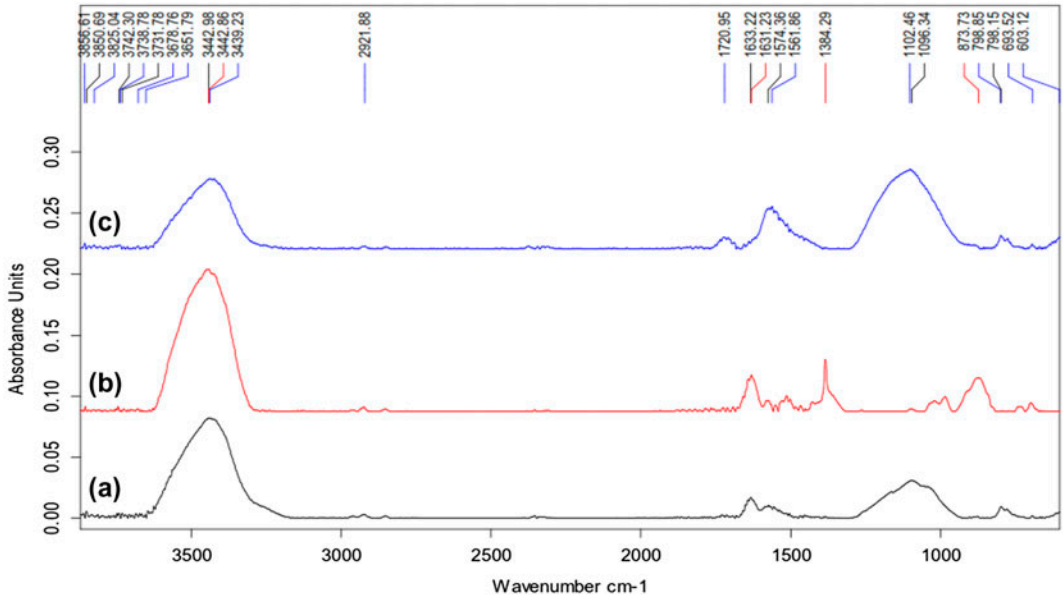

Fig. 3. FT-IR spectra for (a) AC, (b) bare ZnO, and (c) AC–ZnO.

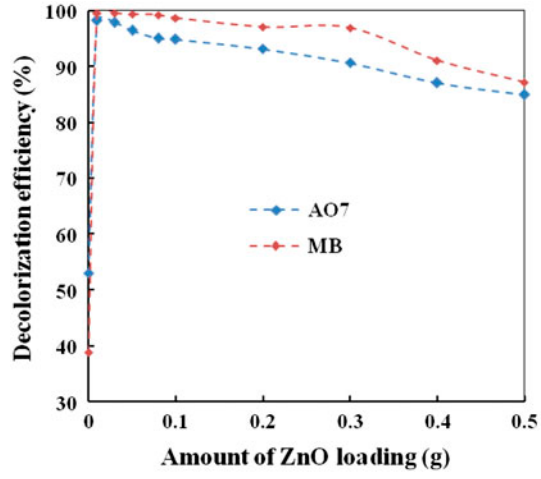

Fig. 4. The effect of various loading rates of ZnO-np in the adsorption of dye with AC–ZnO (dye solution = 50 mg/L, initial pH 7.0, contact time = 240 min, and AC–ZnO conc. = 1.5 g/L).

contact time of 75 min [40]. The optimum contact times of 120 min for MB and 150 min for AO7 were chosen for the subsequent experiments in the present study.

3.3.1. Adsorption kinetics

Adsorption kinetic study is useful to predict the adsorption rate in order to gain the important information for sketching and modeling of the sorption process [41]. Various sorption kinetic models including pseudo-first-order and pseudo-second-order kinetics were applied to the adsorption data. The pseudo-first-order kinetic model is shown by the following equation [6]:

$$\mathrm{Ln}\,(q_e - q_t) = \mathrm{Ln}\,q_e - k_1 t \tag{3}$$

where q_e and q_t (mg/g) are the amount of adsorbed dye at the equilibrium time and at the stated time, respectively. k_1 is the specific rate constant for the first-order kinetic model and t is the contact time. k_1 and q_e are acquired from the slope and intercept of the plotting $\ln(q_e - q_t)$ vs. time (t), respectively. The pseudo-second-order kinetic model is also presented by Eq. (4):

$$\frac{t}{q_t} = \frac{1}{k_2 q_e^2} + \frac{t}{q_e} \tag{4}$$

where k_2 is the specific rate constant of the pseudo-second-order kinetic model and other parameters are the same as the above. k_2 and q_e are calculated from the intercept and slope through plotting t/q_e vs. time (t), as shown in Fig. 5(b), respectively [10]. The values of the kinetic parameters for the sorption are given in Table 2. The results showed that the adsorption kinetic of MB and AO7 onto the AC–ZnO followed the pseudo-second-order kinetic model. The correlation coefficient (R^2) of the pseudo-second-order kinetic model (0.992 for MB and 0.997 for AO7) was found to

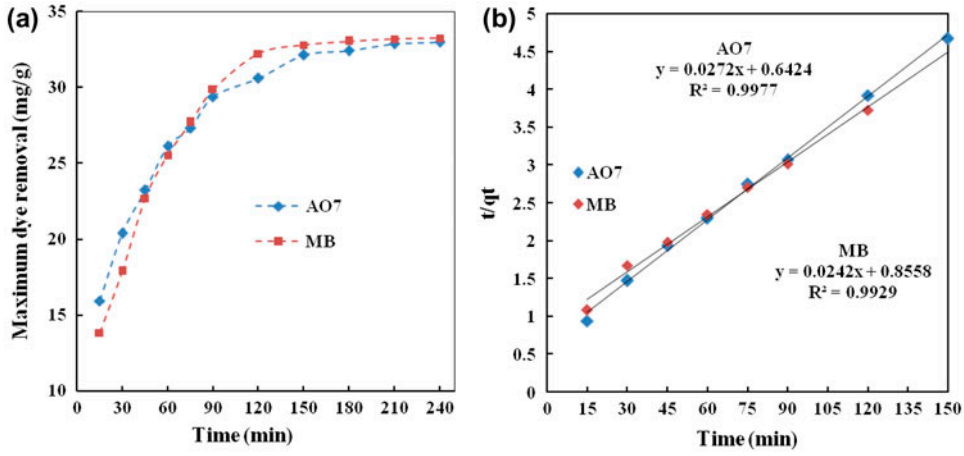

Fig. 5. (a) The effects of contact time on the dye adsorption MB and AO7 by AC–ZnO (dye solution = 50 mg/L, pH 3 for AO7 and 11 for MB, contact time = 240 min and AC–ZnO conc. = 1.5 g/L) and (b) pseudo-second-order kinetic model.

Table 2
Parameters of the kinetic models for MB and AO7 adsorption by AC–ZnO

Adsorbate	Pseudo-first-order model			Pseudo-second-order model		
	k_1	q_e (mg/g)	R^2	k_2	q_e (mg/g)	R^2
MB	0.026	30.56	0.980	0.00050	41.32	*0.992*
AO7	0.022	23.57	0.993	0.00047	30.76	*0.997*

be higher than of the pseudo-first-order kinetic model (Table 2). Similar kinetic results were also reported for the adsorption of dye onto other materials such as ACs coated by palladium, silver, and zinc oxide, and chitosan–zinc oxide nanoparticles [29,35].

3.4. Effect of pH

The influence of solution pH on the sorption of MB and AO7 by AC–ZnO is shown in Fig. 6. The results showed that by increasing the solution pH from 3.0 to 9.0, the removal percentage of MB by the adsorbent remained almost constant and it was increased with increasing the solution pH from 9.0 to 11.0. The high concentration of H^+ ions at lower solution pH can protonate the functional groups of the sorbent and thus the adsorbent become more positively charged [10]. This process can create the repulsive force between cationic MB molecules and positively charged surface of the adsorbent that as a result of it, the dye sorption was finally decreased. Moreover, the competition between positively charged MB and H^+ ions to the sorption, in the lower solution pH, can significantly decrease the removal efficiency of MB by the adsorbent [10]. By increasing solution pH, the active sites on the surface of AC–ZnO, due to the adsorption of OH^- ions, may obtain negative charges which would improve the interaction between the adsorbent and the cationic dye molecules. Therefore, the removal efficiency of MB was increased at the higher pH values. Ozer et al. showed that the maximum adsorption of MB by AC occurred at the solution pH 12 [17]. The adsorption of AO7 by AC–ZnO was increased at pH 3 (91.48%) and its removal percentage was decreased at the higher pH. These results showed that the acidic medium (positively charged surface of the adsorbent) is favorable for the sorption of the anionic dye, AO7. The deprotonation and consequently negatively charged surface of the adsorbent occurred by increasing solution pH; as a result, this phenomenon may cause decrease of AO7 adsorption [4,10,11]. Aber et al. also reported that the maximum removal of AO7 (96.24%) by AC was achieved at pH 2.8 for the initial dye concentration of 150 mg/L [40]. The pH values 11 and 3 were used as the optimum condition to remove MB and AO7, respectively, for the rest of the experiments.

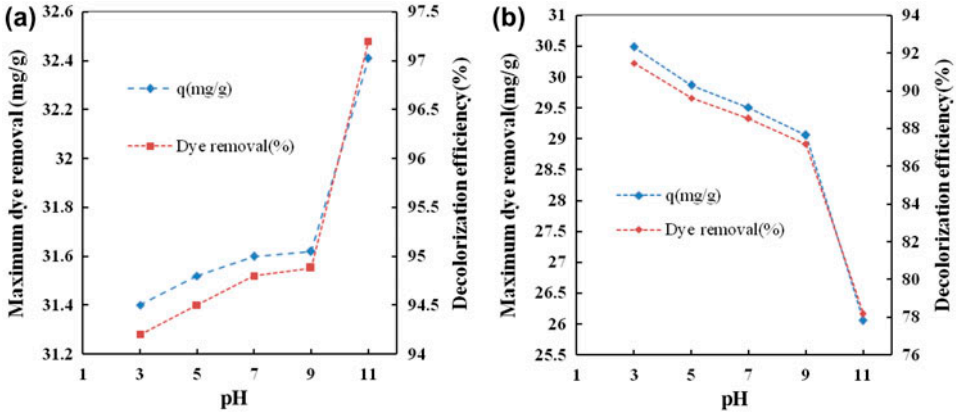

Fig. 6. The effect of pH on the adsorption (a) MB and (b) AO7 by AC–ZnO (dye solution = 50 mg/L, contact time = 120 min for MB and AO7, and AC–ZnO conc. = 1.5 g/L).

3.5. Effect of dye concentration

Fig. 7 shows the effect of various dye concentrations on the adsorption. As seen, by increasing the initial dye concentration from 10 to 150 mg/L, the adsorption capacity of the AC–ZnO was increased (from 6.63 to 65.23 mg/g and from 6.66 to 68.80 mg/g for MB and AO7, respectively). This can be due to the powerful driving force, to overcome the mass transfer resistance, between the aqueous and solid phases that occurs by increasing the initial concentration of the adsorbates [10,12,42].

3.5.1. Adsorption isotherms

The adsorption isotherms represent the adsorbate molecules distribution between the liquid phase and solid phase at the equilibrium state. Three adsorption isotherms including Langmuir, Freundlich, and Dubinin–Radushkevich (D–R) were widely applied for this purpose. The Langmuir adsorption isotherm is based on the assumption that the monolayer adsorption occurs on the homogeneous surface of the adsorbent without interaction between the absorbed molecules [41]. The linearized Langmuir isotherm can be shown by Eq. (5):

$$\frac{C_e}{Q_e} = \frac{1}{bQ_m} + \frac{C_e}{Q_m} \tag{5}$$

where C_e (mg/L) is dye concentration at the equilibrium time and b (l/mg) is the Langmuir constant. q_e (mg/g) and Q_m (mg/g) are the sorption capacity of the adsorbent and the maximum monolayer adsorbent capacity at the equilibrium time, respectively. Q_m and b are achieved from the slope and intercept of linear plot of C_e/q_e vs. C_e, respectively [41].

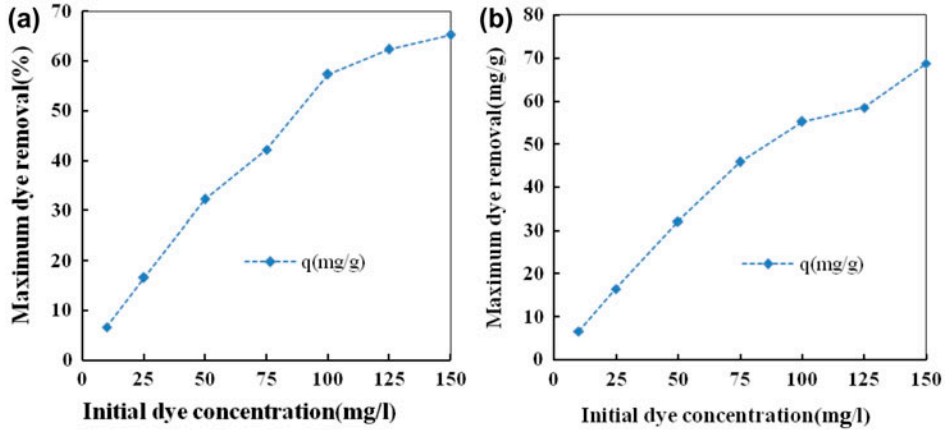

Fig. 7. The effect of dye concentration on the adsorption (a) MB and (b) AO7 by AC–ZnO. (pH 3 for AO7 and 11 for MB, contact time = 120 min for MB and 150 min for AO7, and AC–ZnO conc. = 1.5 g/L).

The Langmuir isotherm parameters and correlation coefficient (R^2) are presented in Table 3. As can be seen, the correlation coefficient of Langmuir isotherm ($R^2 = 0.99$ for MB and 0.98 for AO7) was higher than of Freundlich isotherm's. This indicates that the Langmuir isotherm model fitted the experimental data better than other isotherm models. Ozer et al. found that the sorption of MB onto AC was reasonably well represented by the Langmuir isotherm model [17]. R_L, a separation factor, is used to express the Langmuir isotherm that is calculated by Eq. (6).

$$R_L = \frac{1}{1 + bC_0} \tag{6}$$

where C_0 (mg/L) is the maximum adsorbate concentration in the solution. The R_L values between 0 and 1 show that the sorption process is favorable [29]. In this study, the values of R_L obtained for the sorption of MB and AO7 were approximately 0.01.

The Freundlich isotherm can be used for non-ideal adsorption on heterogeneous surface of the adsorbent that is described by Eq. (7) [43].

$$\log Q_e = \log K_f + \frac{1}{n} \log C_e \tag{7}$$

where K_f (l/g) and n are the isotherm constants which show the capacity and intensity of the adsorption, respectively. K_f and n are determined from the intercept and slope of plotting ln q_e against ln C_e, respectively [43].

The D–R isotherm model is applied to determine the nature of MB and AO7 adsorption by the adsorbent as chemical or physical [43]. The linear form of D–R isotherm can be shown as follows:

$$\log q_e = \log q_m - \beta \varepsilon^2 \tag{8}$$

where q_m (mg/g) is the theoretical saturation sorption capacity based on the isotherm, β (kJ/mol) is related to mean adsorption energy, and ε (Polanyi Potential) is equal to RT ln $(1 + 1/C_e)$. R (kJ/mol K) is the universal gas constant and T (K) is temperature. q_m and β are attained from the intercept and the slope of linear plot of ln q_e vs. ε^2, respectively [43]. E (kJ/mol) is the mean adsorption energy that is obtained from Eq. (9).

$$E = \frac{1}{\sqrt{2\beta}} \tag{9}$$

The E values specify the type of adsorption process. The chemical ion exchange happened for the E value 8–16 kJ/mol. The physical and chemical adsorptions occurred when $E < 8$ and $E > 16$ kJ/mol, respectively [43]. As shown in Table 3, the E values for the adsorption of MB and AO7 onto the AC–ZnO were in the range of 2–4 kJ/mol. Therefore, the sorption process of MB and AO7 by the adsorbent was defined as physical in nature.

3.6. Effect of solution ion strength

The influence of ionic strength on the adsorption is essential, because the dye containing wastewaters generally have a high salt content [11]. Fig. 8 shows the effect of various concentrations of $CaCl_2$ (20–100 mg/L Ca^{+2} ion) on the sorption of MB and AO7 by AC–ZnO. As seen, increasing the solution ion strength even for Ca concentration of 100 mg/L resulted in negligible changes in dye removal by AC–ZnO. This indicates that AC–ZnO could be efficiently used to remove MB and AO7 from high ionic strength aqueous solutions. Li et al. reported that change in solution ionic strength (up to 1 mol/l NaCl) resulted in no significant effect on the removal of MB and reactive red 24 by sludge-based AC [44].

3.7. Effect of temperature

The influence of temperature on the sorption of MB and AO7 through AC–ZnO was determined in the range of 15–45°C. The following equations (Eqs. (10–13)) have been applied to indicate the thermodynamic parameters such as enthalpy (ΔH), Gibbs free energy (ΔG), and entropy (ΔS) [43].

Table 3
Langmuir, Freundlich, and D–R isotherm parameters for the adsorption of dyes onto AC–ZnO

	Langmuir isotherm			Freundlich isotherm			D–R isotherm		
Adsorbate	Q_m (mg/g)	b (l/mg)	R^2	K_f (l/mg)	n	R^2	q_m (mg/g)	E (kJ/mol)	R^2
MB	66.66	0.57	*0.99*	23.57	3.38	0.92	50.90	3.83	0.92
AO7	66.22	0.58	*0.98*	25.79	3.90	0.97	51.41	2.65	0.80

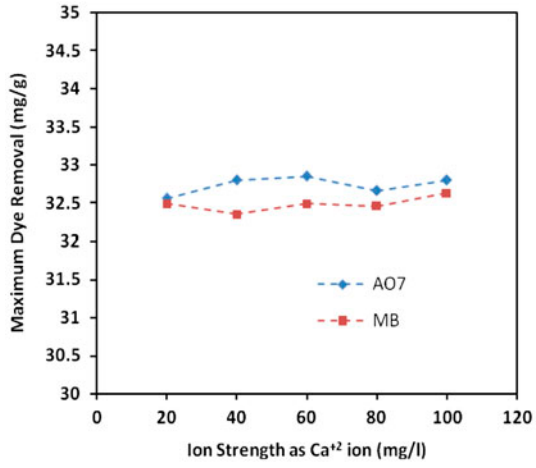

Fig. 8. The effect of solution ion strength on the adsorption of dye by AC–ZnO. (pH 3 for AO7 and 11 for MB, contact time = 120 min for MB and AO7, and AC–ZnO conc. = 1.5 g/L).

$$\Delta G = -RT \ln k \tag{10}$$

$$k = \frac{q_e}{C_e} \tag{11}$$

$$\Delta G = \Delta H - T\Delta S \tag{12}$$

$$\ln k = \frac{\Delta S}{R} - \frac{\Delta H}{RT} \tag{13}$$

where k is the equilibrium constant (obtained from Langmuir isotherm model). The entropy (J/k mol) and enthalpy (kJ/mol) of the sorption were acquired from the intercept and slope of plotting ln k vs. $1/T$, respectively [1]. The thermodynamic parameters are shown in Table 4. The negative values of free energy change (ΔG) at the temperatures of 25–45˚C show that the sorption of the dyes by the adsorbent is thermodynamically spontaneous and feasible, and the sorption process is physical in nature. The ΔG values increased by increasing the temperature; these findings indicate that the higher temperature is favorable for the sorption process [43]. The positive values of enthalpy and entropy for the present work also indicate that the sorption of MB and AO7 by AC–ZnO is endothermic and may indicate an increase in degree of freedom of the adsorbed species [1].

3.8. Regeneration of AC–ZnO

The regeneration of adsorbent is one of the main factors that substantially influences on the sorption process cost. Heating, water, acidic, and basic solutions (sulfuric acid and sodium hydroxide) were used to determine the performance of the spent sorbent. Subsequently, the adsorption experiments were carried out by the regenerated adsorbent to evaluate the regeneration efficiency (R_e), which is calculated using Eq. (14).

Table 4
Thermodynamic parameters for the removal of MB and AO7 by AC–ZnO

Adsorbate	q_e (mg/g)				ΔG (kJ/mol)				ΔH	ΔS
	288 K	298 K	308 K	318 K	288 K	298 K	308 K	318 K	(kJ/mol)	(J/mol K)
MB	26.80	37.98	47.37	64.83	0.781	−1.249	−3.278	−5.307	59.23	202.94
AO7	19.68	33.94	41.53	60.55	1.626	−0.373	−2.373	−4.372	59.21	199.95

Table 5
Adsorption of MB and AO7 onto virgin and regenerated AC–ZnO

Adsorbate	MB		AO7	
	η (%)	R_e (%)	η (%)	R_e (%)
AC–ZnO (virgin)	99.66	–	96.40	–
AC–ZnO (heating)	96.66	100	96.40	100
AC–ZnO (sulfuric acid)	93.24	96.52	89.76	92.91
AC–ZnO (sodium hydroxide)	80.96	83.85	73.64	76.23
AC–ZnO (distilled water)	78.62	81.38	88.86	91.98

$$R_e = \frac{M_{ac}}{M_{bc}} \quad (14)$$

where M_{bc} and M_{ac} are quantities of dye adsorbed by AC–ZnO before and after regeneration, respectively [1].

The results of MB and AO7 sorption through virgin and regenerated AC–ZnO are shown in Table 5. As seen, the regeneration via heating (200˚C for 60 min) and sulfuric acid (10% v/v solution) was the best methods for desorption of dyes onto the adsorbent. The removal efficiency (η) of dyes by heating regenerated AC–ZnO was the same as the virgin sorbent. The regeneration efficiency (R_e) using heating was 100% for both the dyes. The R_e value also using sulfuric acid was 96.52 and 92.91% for MB and AO7, respectively. Foo and Hameed showed that the removal efficiency of microwave heating-regenerated AC for MB dye, even after five adsorption–regeneration cycles, toward the virgin AC was 75.41–76.69% [45]. Regeneration with distilled water for AO7-saturated adsorbent was also showed that water has a high performance in desorption of AO7 onto the adsorbent. The data can be considered as a suggestion for the industrial applications of AC–ZnO for the dyes removal from aqueous solutions.

4. Conclusion

The AC–ZnO, as an adsorbent, was used to remove MB and AO7 from aqueous solutions. The optimum contact times for the removal of MB (32.22 mg/g) and AO7 (32.13 mg/g) by AC–ZnO were obtained during 120 min and 150 min, respectively. Moreover, the optimum pH was achieved at pH 11 for MB and pH 3 for AO7. The Langmuir isotherm model and pseudo-second-order kinetic model described the data better than other isotherm and kinetic models. The thermodynamic study, especially at the temperatures of 25–45˚C, showed that the sorption of the dyes by the adsorbent is spontaneous, feasible, and the sorption process is physical in nature. The results also showed that sulfuric acid solution and heating can effectively recover the adsorbed dyes from the dyes-saturated AC–ZnO. It is clear that AC–ZnO, in comparison with raw AC, was more efficient sorbent for the removal of MB and AO7 and it can be proposed for the removal of these dyes from aqueous solutions.

Acknowledgment

This study was supported by the vice chancellery for Research of Ilam University of Medical Sciences, Iran (Grant No. 924018.58).

References

[1] H. Nourmoradi, M. Nikaeen, M. Khiadani, Removal of benzene, toluene, ethylbenzene and xylene (BTEX) from aqueous solutions by montmorillonite modified with nonionic surfactant: Equilibrium, kinetic and thermodynamic study, Chem. Eng. J. 191 (2012) 341–348.
[2] P. Muthirulan, M. Meenakshisundararam, N. Kannan, Beneficial role of ZnO photocatalyst supported with porous activated carbon for the mineralization of alizarin cyanin green dye in aqueous solution, J. Adv. Res. 4 (2013) 479–484.
[3] A.M.M. Vargas, A.L. Cazetta, M.H. Kunita, T.L. Silva, V.C. Almeida, Adsorption of methylene blue on activated carbon produced from flamboyant pods (Delonix regia): Study of adsorption isotherms and kinetic models, Chem. Eng. J. 168 (2011) 722–730.
[4] L. Jayalakshmi, V. Devadoss, K. Ananthakumar, Adsorption of acid orange-7 dye onto activated carbon produced from bentonite-A study of equilibrium adsorption isotherm, Chem. Sci. Trans. 2 (2013) S7–S12.
[5] Y. Li, Q. Du, T. Liu, X. Peng, J. Wang, J. Sun, Y. Wang, S. Wu, Z. Wang, Y. Xia, Comparative study of methylene blue dye adsorption onto activated carbon, graphene oxide, and carbon nanotubes, Chem. Eng. Res. Des. 91 (2013) 361–368.
[6] M.N. Ashiq, M. Najam-Ul-Haq, T. Amanat, A. Saba, A.M. Qureshi, M. Nadeem, Removal of methylene blue from aqueous solution using acid/base treated rice husk as an adsorbent, Desalin. Water Treat. 49 (2012) 376–383.
[7] J. Fernandez, P. Maruthamuthu, A. Renken, J. Kiwi, Bleaching and photobleaching of orange II within seconds by the oxone/Co^{2+} reagent in Fenton-like processes, Appl. Catal., B 49 (2004) 207–215.
[8] N. Daneshvar, S. Aber, F. Hosseinzadeh, Study of CI acid orange 7 removal in contaminated water by photo oxidation processes, Global Nest J. 16 (2008) 16–23.
[9] A. Rahmani, M. Zarrabi, M. Samarghandi, A. Afkhami, H. Ghaffari, Degradation of azo dye reactive black 5 and acid orange 7 by Fenton-like mechanism, Int. J. Chem. Eng. 7 (2010) 87–94.
[10] L. Zhang, H. Zhang, Y. Tian, Z. Chen, L. Han, Adsorption of methylene blue from aqueous solutions onto sintering process red mud, Desalin. Water Treat. 47 (2012) 31–41.
[11] F. Gholami-Borujeni, A.H. Mahvi, S. Nasseri, M.A. Faramarzi, R. Nabizadeh, M. Alimohammadi, Enzymatic treatment and detoxification of acid orange 7 from textile wastewater, Appl. Biochem. Biotechnol. 165 (2011) 1274–1284.
[12] M. Ghaedi, M.N. Biyareh, S.N. Kokhdan, S. Shamsaldini, R. Sahraei, A. Daneshfar, S. Shahriyar, Comparison of the efficiency of palladium and silver nanoparticles loaded on activated carbon and zinc oxide nanorods loaded on activated carbon as new adsorbents for removal of congo red from aqueous solution: Kinetic and isotherm study, Mater. Sci. Eng., C 32 (2012) 725–734.
[13] A. Mittal, D. Jhare, J. Mittal, Adsorption of hazardous dye eosin yellow from aqueous solution onto waste material de-oiled soya: Isotherm, kinetics and bulk removal, J. Mol. Liq. 179 (2013) 133–140.

[14] A. Mittal, V. Thakur, J. Mittal, H. Vardhan, Process development for the removal of hazardous anionic azo dye congo red from wastewater by using hen feather as potential adsorbent, Desalin. Water Treat. 52 (2014) 1–11.
[15] Y. Liu, X. Zhao, J. Li, D. Ma, R. Han, Characterization of bio-char from pyrolysis of wheat straw and its evaluation on methylene blue adsorption, Desalin. Water Treat. 46 (2012) 115–123.
[16] V. Vadivelan, K.V. Kumar, Equilibrium, kinetics, mechanism, and process design for the sorption of methylene blue onto rice husk, J. Colloid Interface Sci. 286 (2005) 90–100.
[17] C. Ozer, M. Imamoglu, Y. Turhan, F. Boysan, Removal of methylene blue from aqueous solutions using phosphoric acid activated carbon produced from hazelnut husks, Toxicol. Environ. Chem. 94 (2012) 1283–1293.
[18] M. Hejazifar, S. Azizian, Adsorption of cationic and anionic dyes onto the activated carbon prepared from grapevine rhytidome, J. Dispersion Sci. Technol. 33 (2012) 846–853.
[19] O.S. Bello, I.A. Adeogun, J.C. Ajaelu, E.O. Fehintola, Adsorption of methylene blue onto activated carbon derived from periwinkle shells: Kinetics and equilibrium studies, Chem. Ecol. 24 (2008) 285–295.
[20] M. Samarghandi, M. Hadi, S. Moayedi, F.B. Askari, Two-parameter isotherms of methyl orange sorption by pinecone derived activated carbon, Iran. J. Environ. Health Sci. Eng. 6 (2009) 285–294.
[21] Y.S. Ho, G. McKay, Sorption of dye from aqueous solution by peat, Chem. Eng. J. 70 (1998) 115–124.
[22] G. Mc Kay, H. Blair, J. Gardner, Rate studies for the adsorption of dyestuffs onto chitin, J. Colloid Interface Sci. 95 (1983) 108–119.
[23] S. Keleşoğlu, M. Kes, L. Sütçü, H. Polat, Adsorption of methylene blue from aqueous solution on high lime fly ash: Kinetic, equilibrium, and thermodynamic studies, J. Dispersion Sci. Technol. 33 (2012) 15–23.
[24] H. Chen, J. Zhao, A. Zhong, Y. Jin, Removal capacity and adsorption mechanism of heat-treated palygorskite clay for methylene blue, Chem. Eng. J. 174 (2011) 143–150.
[25] Z. Aksu, S. Ertuğrul, G. Dönmez, Methylene blue biosorption by *Rhizopus arrhizus*: Effect of SDS (sodium dodecylsulfate) surfactant on biosorption properties, Chem. Eng. J. 158 (2010) 474–481.
[26] Z. Li, P.-H. Chang, W.-T. Jiang, J.-S. Jean, H. Hong, Mechanism of methylene blue removal from water by swelling clays, Chem. Eng. J. 168 (2011) 1193–1200.
[27] M. Qiu, Q. Jian, D. Yu, K. Feng, Removal of methylene blue using acid and heat treatment of clinoptilolite, Desalin. Water Treat. 24 (2010) 61–66.
[28] M.I. El-Khaiary, F.A. Gad, M.S. Mahmoud, H. El-Din Samy, Adsorption of methylene blue from aqueous solution by chemically treated water hyacinth, Toxicol. Environ. Chem. 91 (2009) 1079–1094.
[29] R. Salehi, M. Arami, N.M. Mahmoodi, H. Bahrami, S. Khorramfar, Novel biocompatible composite (chitosan–zinc oxide nanoparticle): Preparation, characterization and dye adsorption properties, Colloids Surf., B 80 (2010) 86–93.
[30] E. Haque, J.W. Jun, S.H. Jhung, Adsorptive removal of methyl orange and methylene blue from aqueous solution with a metal-organic framework material, iron terephthalate (MOF-235), J. Hazard. Mater. 185 (2011) 507–511.
[31] V. Garg, M. Amita, R. Kumar, R. Gupta, Basic dye (methylene blue) removal from simulated wastewater by adsorption using Indian Rosewood sawdust: A timber industry waste, Dyes Pigm. 63 (2004) 243–250.
[32] G.O. El-Sayed, Removal of methylene blue and crystal violet from aqueous solutions by palm kernel fiber, Desalination 272 (2011) 225–232.
[33] C.-H. Weng, Y.-T. Lin, T.-W. Tzeng, Removal of methylene blue from aqueous solution by adsorption onto pineapple leaf powder, J. Hazard. Mater. 170 (2009) 417–424.
[34] M. Doğan, M. Alkan, Y. Onganer, Adsorption of methylene blue from aqueous solution onto perlite, Water Air Soil Pollut. 120 (2000) 229–248.
[35] M. Ghaedi, M. Ghaedi, S.N. Kokhdan, R. Sahraei, A. Daneshfar, Palladium, silver, and zinc oxide nanoparticles loaded on activated carbon as adsorbent for removal of bromophenol red from aqueous solution, J. Ind. Eng. Chem. 19 (2013) 1209–1217.
[36] A. Changsuphan, M.I. Wahab, N.T. Kim Oanh, Removal of benzene by ZnO nanoparticles coated on porous adsorbents in presence of ozone and UV, Chem. Eng. J. 181 (2012) 215–221.
[37] A. Akyol, M. Bayramoğlu, Photocatalytic degradation of remazol red F3B using ZnO catalyst, J. Hazard. Mater. 124 (2005) 241–246.
[38] B. Hameed, A. Ahmad, N. Aziz, Isotherms, kinetics and thermodynamics of acid dye adsorption on activated palm ash, Chem. Eng. J. 133 (2007) 195–203.
[39] J. Chen, X. Wen, X. Shi, R. Pan, Synthesis of zinc oxide/activated carbon nano-composites and photodegradation of rhodamine B, Environ. Eng. Sci. 29 (2012) 392–398.
[40] S. Aber, N. Daneshvar, S.M. Soroureddin, A. Chabok, K. Asadpour-Zeynali, Study of acid orange 7 removal from aqueous solutions by powdered activated carbon and modeling of experimental results by artificial neural network, Desalination 211 (2007) 87–95.
[41] H. Faghihian, H. Nourmoradi, M. Shokouhi, Removal of copper (II) and nickel (II) from aqueous media using silica aerogel modified with amino propyl triethoxysilane as an adsorbent: Equilibrium, kinetic, and isotherms study, Desalin. Water Treat. 52 (2014) 305–313.
[42] C.O. Ijagbemi, J.I. Chun, D.H. Han, H.Y. Cho, S.J. O, D.S. Kim, Methylene blue adsorption from aqueous solution by activated carbon: Effect of acidic and alkaline solution treatments, J. Environ. Sci. Health., Part A 45 (2010) 958–967.
[43] H. Nourmoradi, M. Khiadani, M. Nikaeen, Multicomponent adsorption of benzene, toluene, ethylbenzene, and xylene from aqueous solutions by montmorillonite modified with tetradecyl trimethyl ammonium bromide, J. Chem. 2013 (2013) 1–10.
[44] W.H. Li, Q.Y. Yue, B.Y. Gao, Z.H. Ma, Y.J. Li, H.X. Zhao, Preparation and utilization of sludge-based activated carbon for the adsorption of dyes from aqueous solutions, Chem. Eng. J. 171 (2011) 320–327.
[45] K. Foo, B. Hameed, A rapid regeneration of methylene blue dye-loaded activated carbons with microwave heating, J. Anal. Appl. Pyrolysis 98 (2012) 123–128.